Waste Management 203 (2025) 114895

Contents lists available at ScienceDirect

Waste Management

journal homepage: www.elsevier.com/locate/wasman

Research Paper

Microbial acclimation of thermophilic anaerobic digestate enhances biogas production and biodegradation of polylactic acid in combination with the organic fraction of municipal solid waste (OFMSW)

Hager Galal Elsayed Elboghdady [a], Elisa Clagnan [a,*], Veronica De Franceschi [a], Mirko Cucina [b], Marta Dell'Orto [a], Patrizia De Nisi [a], Andrea Goglio [a], Fabrizio Adani [a]

[a] Gruppo Ricicla labs., Department of Agricultural and Environmental Sciences - Production, Territory, Agroenergy (DiSAA), University of Milan (Università degli Studi di Milano), Via Celoria 2, 20133 Milano, Italy
[b] National Research Council of Italy, Institute for Agriculture and Forestry Systems in the Mediterranean (CNR-ISAFOM), Via della Madonna Alta 128, 06128 Perugia, Italy

ARTICLE INFO

Keywords:
Anaerobic digestion
Biogas
Bioplastic
Microbial acclimation
Organic fraction municipal solid waste (OFMSW)
Polylactic acid (PLA)

ABSTRACT

Bioplastics are a promising alternative to conventional plastics. Their anaerobic co-digestion with the organic fractions of municipal solid waste (OFMSW) is an ideal end-of-life scenario reducing pre-treatment and increasing efficiency and biogas production. Bioplastic degradation is limited under anaerobic digestion (AD) as it requires longer hydraulic retention time (HRT) compared to industrial OFMSW plants' HRTs. Here, three AD runs were conducted sequentially under thermophilic conditions to investigate the effects of inoculum acclimation on enhancing the degradation of polylactic acid (PLA) and OFMSW in mono and co-digestion (PLA + OFMSW). In PLA mono-digestion, microbial acclimation increased biogas production up to +152 % (831 ± 11 NL $kgVS^{-1}$) and biogas production rate from 27 to 47 NL $kgVS^{-1}$ d^{-1} with a 5-day reduction of the lag phase. This improvement was associated with the enrichment of the PLA-degrading bacteria *Tepidanaerobacter*. In PLA + OFMSW co-digestion, biogas production increased of +69 % (827 ± 69 NL $kgVS^{-1}$), the biogas production rate increased to 58 NL $kgVS^{-1}$ d^{-1} with a lag phase reduction of 7 days. An increase of both protein degraders (*Halocella* and *Acetomicrobium*) and *Tepidanaerobacter* was achieved. In OFMSW mono-digestion, acclimation increased cumulative biogas production to + 22 % (719 ± 25 NL $kgVS^{-1}$) with no biogas production rate and lag phase modifications, indicating an already adapted community. A variance in *Methanothermobacter* and *Metanoculleus* abundances across treatments was linked to different biomethane productions. Microbial acclimation is a valid and economical approach to enhance biogas production and PLA degradability, alone or with OFMSW, further reducing HRTs enabling sustainable bioplastic and OFMSW waste management.

1. Introduction

Bioplastics are emerging as a viable alternative to conventional petroleum-based plastics and currently, they account for ~0.5 % of plastics produced annually. The annual production of bioplastics is expected to increase by 66 % by 2029 (European Bioplastics, 2024). PLA is the most commercially available bioplastic and accounts for 37.1 % of global bioplastics production in 2024 and expected to increase to 42.3 % by 2029 (European Bioplastics, 2024). PLA is used in the manufacturing of consumer goods and disposable products such as cutlery, glasses, dishes, and packaging, but also in construction, agriculture, medical applications, and fibre production (Cucina et al., 2021a). Currently, bioplastic waste is usually collected with the OFMSW and as a result, the content of bioplastics in the waste can potentially reach the concentrations of 8–10 % of OFMSW by weight, posing the problems of bioplastic waste management, degradation, and leakage in the environment (Cucina et al., 2021b). In the context of circular economy, the increasing production of PLA needs therefore to be combined with a suitable waste management system to improve bioplastic sustainability.

Among the possible end-of-life scenarios, AD is a promising technology for bioplastic biodegradation (Abraham et al., 2021, Cucina et al., 2021a). Anaerobic digestion is typically used to process various

* Corresponding author.
E-mail address: Elisa.Clagnan@unimi.it (E. Clagnan).

https://doi.org/10.1016/j.wasman.2025.114895
Received 25 January 2025; Received in revised form 1 May 2025; Accepted 14 May 2025

types of waste such as OFMSW, at both mesophilic (35–37 °C) or thermophilic (50–60 °C) temperatures (Samoraj et al., 2022), to produce biomethane and digestate (or compost) that can be further used as an energy source and bio-based fertilizer, respectively (Kumar and Samadder, 2020). Currently, in AD plants, all plastics (and as a consequence bioplastics) are de-packaged to avoid clogging of the system and the production of a digestate containing microplastics (Cazaudehore et al., 2023a; Taneepanichskul et al., 2022). This de-packaging process results in a significant loss of OFMSW, which reduces the profitability of AD (Cazaudehore et al., 2023a). Furthermore, hypothesising an absence of plastics within the OFMSW waste, an optimised co-digestion of bioplastics and OFMSW will eliminate the need for sorting and separating, thereby reducing the overall costs associated with the AD process. Industrial AD plants treat OFMSW normally at short hydraulic retention times (HRTs), i.e. between 15 and 30 days (Cazaudehore et al., 2022c). On the other hand, PLA needs longer HRTs to be completely degraded under mesophilic and thermophilic conditions, which are not compatible with the HRTs used for OFMSW. Cazaudehore et al. (2023b) assessed the degradability of PLA-based material in AD at 38 °C and 58 °C achieving a degradation of 75 % in 500 and 100 days, respectively. Other studies reported no degradation of PLA after 60 days at 38 °C, while 93 % degradation was achieved at 58 °C in 120 days (Jin et al., 2022). These data indicate that both thermophilic conditions and long HRTs promote PLA degradation. Thermophilic conditions are more performant since PLA reaches its glass transition (i.e., polymeric structure changes from crystalline to amorphous) at high temperatures, becoming more accessible to microbial activity and leading to a higher polymer biodegradability (Cazaudehore et al., 2021; Cucina et al., 2021b). However, even with the transition to an amorphous structure, PLA biodegradation can hardly meet industrial OFMSW HRTs.

In terms of co-digestion, a recent study investigating the degradation of PLA with kitchen waste (KW) at 55 °C reported a production of 693 ± 10 L CH_4 $kgVS^{-1}$ under thermophilic conditions after 30 days, while the theoretical CH_4 potential of PLA (100 % PLA degradation) (i.e., 1092 ± 8 L CH_4 $kgVS^{-1}$) was reached after 120 days (Lu et al., 2022). El-Mashad et al. (2012) observed no biogas production over 43 days from PLA-based cups alone in a co-digestion with food waste at 50 °C, when changing the substrate form cups to PLA-based straws a 0.024 L gVS^{-1} production was achieved. Both studies seem to indicate that PLA did not degrade entirely until food waste completely degraded. It is therefore necessary to further research methodologies to shorten PLA's HRTs and to enable PLA and OFMSW co-digestion and improve AD's workflow, process, microbiology, and end-products quality. To overcome HRT limitations of PLA in both mono and co-digestion, various strategies can be used, such as PLA pre-treatments, the addition of additives to PLA, inoculum acclimatization or bioaugmentation (Cazaudehore et al., 2022a). Acclimatization has been successfully applied to AD of various organic wastes (e.g. olive mill effluent and extruded food waste) to improve degradability and CH_4 production (Gonçalves et al., 2011). Recently, inoculum acclimatization was successfully applied to PLA mono-digestion under thermophilic conditions, leading to an increase of PLA-degradation by 97 % compared to a non-acclimated inoculum (from 395 to 779 NL $kgVS^{-1}$ of biogas) (Clagnan et al., 2023). Nevertheless, little is known about the bacterial and archaeal communities that lead to bioplastic degradation in AD, especially during acclimatization. Understanding the composition of these microbial consortia is crucial to improve biodegradability of bioplastics in AD and achieve a more efficient co-digestion with OFMSW (Peng et al., 2022).

In this context, this study aims at investigating the effects of microbial communities' acclimatization on PLA mono- and co-digestion with OFMSW, therefore using acclimatization as a low-cost approach to improve PLA degradation. Main objectives were to: *i.* acclimatize digestate microbial communities to PLA and OFMSW under thermophilic anaerobic mono- and co-digestion through a series of batch runs; *ii.* investigate the effect of acclimatization on biodegradation rate and biogas production, and *iii.* characterize the bacterial and archaeal community structure to identify the microbial drivers of acclimatization.

2. Materials and methods

2.1. Substrates: inoculum, OFMSW and PLA

The digestates used as inocula were collected from a full-scale AD plant that treats OFMSW operating under thermophilic conditions (55 ± 2°C) (Lombardy Region, Italy). Within this plant, bioplastic is mechanically separated from the OFMSW on arrival. OFMSW is then processed by a bio-pulper (mechanical pulping) to reach a slurry-like final product that is then anaerobically digested. Digestate was collected across Spring 2023 before each AD run and immediately sieved with a 2 mm mesh to retain possible undigested materials. The digestate was then pre-incubated at 55 ± 2°C until no biogas production was detected.

Pulped OFMSW was sampled from the same plant from which digestate was sampled once at the beginning of the experimental period. After sieving with a 2 mm mesh the OFMSW was stored at −80 °C. Frozen OFMSW was then defrosted when needed and used across the whole experimental period as OFMSW substrate. Digestates and OFMSW were characterized for total solids (TS), volatile solids (VS), pH, total organic carbon (TOC), total ammonium nitrogen (NH_4^+-N), volatile fatty acids (VFA), total alkalinity (TA), and the ratio of VFA to TA here referred as FOS/TAC (see section 2.3).

PLA-based cups, labelled as compostable by TÜV Austria (Austria), were purchased from an Italian supermarket (Milan, Lombardy Region, Italy). The PLA cups were then cut into 2.5 × 2.5 cm squares as recommended by standard tests for the assessment of anaerobic degradability of bioplastics (ISO 14855-2, 2018) and used as PLA substrate.

2.2. Batch test experimental design

Three AD runs were conducted sequentially to achieve inoculum acclimation and assess its efficiency of PLA degradation with and without OFMSW. All AD runs were operated under thermophilic conditions (55 ± 2°C) using 500 mL glass bottles filled with digestate (300 g) and substate. Bottles were manually shacked daily to ensure optimal mixing. Five treatments were set up: (1) PLA mono-digestion (PLA): digestate plus PLA (3 g fresh weight (FW)); (2) PLA and OFMSW co-digestion (PLA + OFMSW): digestate plus PLA (1.5 g FW) and OFMSW (6.3 g FW) with PLA representing 50 % on a carbon basis of the total substrate; (3) OFMSW mono-digestion (OFMSW): digestate plus OFMSW (12.6 g FW); (4) digestate as negative control; and (5) digestate plus microcrystalline cellulose (3 g FW) as positive control. Substrate quantities were selected to ensure a carbon ratio between the substrate and digestate of 0.33 according to Cucina et al. (2021b), Cucina et al. (2022). Although the inoculum-to-substrate ratio (ISR) was initially calculated based on fresh weight following the protocol previously established in (Clagnan et al., 2023), ISR values were also recalculated using VS to align with common reporting standards in anaerobic digestion research (Table S1).

Bottles were purged with pure N_2 for 1 min to ensure an anaerobic environment and tightly capped before the beginning of each run.

For the first AD run, all the bottles were placed at 55 ± 2 °C in a static incubator. Three replicates were used for each treatment while five for PLA and PLA + OFMSW; these two additional bottles were used as controls to track residual biogas production across the three runs. After the first run, all bottles were opened and the digestate from PLA and PLA + OFMSW treatments were sieved to 2 mm to retain eventual plastic residues (none retrieved). Replicates of each treatment were then mixed and used both as inoculum for the second run and characterization analyses.

For the second AD run, four bottles were filled with 150 mL of digestate coming from the first AD run, 150 mL of fresh digestate and the same substrate weights from the previous run were adopted. A fifth bottle was kept as a control without any substrate addition to check the

background methane production of potential PLA residues in the digestate after run 1. This control will be eliminated at the end of run 2. For run 3, only three replicates were used, following the same protocol proposed for the second run with a fourth bottle maintained as a control.

Although batch runs have been performed keeping constant all variables, fresh inoculum taken directly from full scale plant before each run could be different affecting AD processes (Table 1). To account for this variability and ensure data comparability across different runs, all runs have been carried on until maximum cellulose biogas production was achieved, i.e. 600 NL kgVS^{-1} (Clagnan et al., 2023).

Bottles were regularly analysed to determine biogas production both quantitatively and qualitatively. The volume of biogas produced was measured by withdrawing gas with a 100-mL syringe (Chickering et al., 2018). Biogas production of blank and control bottles was subtracted from the biogas production of every sample. Biogas composition was analysed through gas chromatography (Agilent Technologies 3000A 2-channel Micro GC (G2801A, USA)) twice a week.

Digestate samples collected at the end of each run were then used for chemical (TS, VS, VFA, TA, TOC, and NH_4^+-N) characterization (see section 2.3).

2.3. Chemical characterisation

Digestates were characterized before and after each AD run (Tables 1 and 2). Chemical analyses on digestates and substrates were carried out following standard procedures; TS and VS were determined according to standard procedures of the American Public Health Association (Rice et al., 2017). TOC was analysed using COD 15,000 test kits (range of 1.0–15.0 g LO_2^{-1}) (Nanocolor, Macherey Nagel, Germany) and then converted to C by stoichiometric calculations. pH was determined using a pH-meter (Eutech ™ pH 700, Thermo Fisher Scientific, Waltham, MA, USA). Ammonium-N was measured with the Nanocolor Ammonium100 (4–80 mg L^{-1} NH_4^+-N) kit (Nanocolor, Macherey Nagel, Germany), and absorbance was measured with a PF-12 Plus photometer (Macherey Nagel, Germany) using the supernatant layer of each sample after centrifugation at 6000 rpm for 15 min (Chiappero et al., 2021). VFA, TA and FOS/TAC were determined by titration as described by Di Maria et al. (2014).

All chemical analyses were conducted in triplicate. Averages and standard deviations were calculated through Microsoft Excel 2021 and its analysis toolbox. Significant differences for normal parameters were determined using analysis of variance (ANOVA) followed by the Tukey test using SPSS version 29.1 software.

Table 1
Chemical characterization of inoculum and substrates.

Parameter	Digestate Run 1	Run 2	Run 3	OFMSW	PLA
Total solids (%)	5[a] ± 0b[b]	5 ± 0.1b	4.1 ± 0.1a	17.2 ± 0.3	99.4 ± 0.0
Volatile solids (% dry matter)	56.9 ± 0.1a	49.5 ± 2.3a	55.6 ± 1.6a	86.3 ± 0.1	100 ± 0.0
Total organic C (% dry matter)	20.6 ± 2.7a	25.2 ± 0.5ab	28.1 ± 0.1b	58.1 ± 4.6	
pH	8.6 ± 0.0a	9.3 ± 0.0b	8.5 ± 0.0a	6.1 ± 0.0	
Titrable acidity ($gCH_3COOH\ L^{-1}$)	1.8 ± 0.9a	4.2 ± 0.4b	1.8 ± 0.4a	3.2 ± 0.5	
Total alkalinity ($gCaCO_3\ L^{-1}$)	27.8 ± 0.3a	30.6 ± 0.8a	35.9 ± 0.8b	9.9 ± 0.0	
FOS/TAC	0.31 ± 0.2a	0.48 ± 0.1a	0.24 ± 0.1a	1.6 ± 0.3	
Ammonium-N ($gN\text{-}NH_3\ L^{-1}$)	3 ± 0.1a	3 ± 0.1a	2.9 ± 0.1a	0.4 ± 0.1	

[a] Av. ± St. Dev. (n = 3).
[b] Letters indicate statistical differences ($p \leq 0.05$) across the three runs digestates for each parameter according to Tukey test.

2.4. Kinetic analysis and calculations

A modified Gompertz model was applied to determine the kinetic parameters of biogas production potential of the substrates for each run (Mu et al., 2021). Maximum biogas production rates (R_{max}) and lag phases (λ) were calculated from experimental data and subsequently applied in the following equation to evaluate the model's suitability:

$$G(t) = B0 \times exp\left(-exp\left(\frac{R_{max} \times e}{B0} \times (\lambda - t) + 1\right)\right)$$

where G(t) is the cumulative biogas production (NL kgVS^{-1}), B0 is the biogas production potential (NL kgVS^{-1}), R_{max} is the maximum biogas production rate (NL kgVS^{-1} d^{-1}), λ is the lag phase (days), t is the digestion time (days), and e = 2.7183.

B0 parameters were taken from literature assuming that batch experiments were carried out under optimal conditions. As reported in Section 2.2., to confirm optimal environmental conditions, cellulose was used as positive control. Under optimal conditions, cellulose total production is 600 NL kgVS^{-1}. Fig. S1 shows that cellulose degradation reached plateau, and that experimental data had a good fitting to model curves (i.e., $R^2 = 0.974$); it can be therefore assumed that all runs were performed under optimal environmental conditions. The selected model and B0 were thus used if model fitting parameters where higher than literature ($R^2 = 0.967$) if inhibition occurred ($R < 0.967$) data were excluded for kinetics application, as reported in the Section 3.1.).

To build the model,B0 (the biogas production potential) for PLA in mono-digestion was estimated as the average (i.e. av. 840 L kgVS^{-1}) of the biogas productions reported by Bernat et al. (2021), where PLA-based cups were anaerobically digested at 58 °C under different organic loading rates. These data were chosen over the commonly used theoretical biogas values calculated by using the Buswell equation for pure PLA (934 L kgPLA^{-1}) at 35 °C and 1 atm (Buswell and Mueller, 1952) as the Buswell equation does not account for the use of substrate, and/or other pathways of conversion of organic material, for bacterial biomass production (de Lemos Chernicharo, 2007). It is assumed that 10 % of the total carbon contained in the polymer is utilised for bacteria biomass production (García-Depraect et al., 2023) and therefore that this 10 % does not contribute to the theoretical biogas yield value as calculated by Buswell equation. The use of the Buswell equation was therefore discarded as it would have led to an overestimation of the theoretical biogas yield.

For the calculation of the B0 of OFMSW, the maximum biogas production was estimated as the average (i.e. av. 755 ± 68 (n = 6)) of the anaerobic bio-gasification potential (ABP) data obtained from different OFMSW samples collected from various plants across the Lombardy region in Italy (Schievano et al., 2009; Tambone et al., 2010).

The B0 for the co-digestion treatment was calculated by multiplying the cumulative biogas production of the mono-digestion treatments previously described by the corresponding VS percentage of each substrate added in the co-digestion treatment.

To investigate the effects of co-digestion on the degradability of PLA and biogas production, theoretical cumulative biogas productions were calculated for each run of co-digestion by using the cumulative biogas production obtained from PLA and OFMSW mono-digestions within the following equation:

$$B_{co} = (B_{PLA} V_{PLA}) + (B_{OFMSW} V_{OFMSW})$$

where B_{co} is the theoretical biogas production of co-digestion (NL kgVS^{-1}), B_{PLA} is the biogas production of PLA mono-digestion (NL kgVS^{-1}), V_{PLA} is the amount of VS of PLA added within a bottle (g VS), Bo_{FMSW} is the biogas production of OFMSW mono-digestion (NL kgVS^{-1}), and V_{OFMSW} is the amount of VS of OFMSW added within a bottle (g VS).

Table 2
Digestate characterization at the end of each run.

Parameter	Run 1				Run 2				Run 3			
	Cellulose	OFMSW	PLA	PLA + OFMSW	Cellulose	OFMSW	PLA	PLA + OFMSW	Cellulose	OFMSW	PLA	PLA + OFMSW
Total solids (%)	3.6 [a] ± 0a[b]	3.9 ± 0.5a	3.7 ± 0a	3.8 ± 0.2a	3.6 ± 0a	3.2 ± 0.4a	3.5 ± 0.1a	3.5 ± 0a	3.7 ± 0.1a	3.7 ± 0.4a	3 ± 0.1a	3.2 ± 0a
Volatile solids (% dry matter)	53.1 ± 0.3a	61.4 ± 13.6a	51.1 ± 0.4a	54.1 ± 2.4a	50.1 ± 0.6a	50.2 ± 0.1a	51 ± 0a	47.3 ± 2.5a	54.9 ± 0.2a	49.9 ± 1.8a	49.7 ± 0.4a	44.8 ± 7a
Total organic C (% dry matter)	41.9 ± 0.4a	39.6 ± 0a	37 ± 4.3a	46.4 ± 2.5a	35.9 ± 1.5a	36 ± 0.4a	34 ± 2a	35.4 ± 0.8a	54.9 ± 0.2a	49.9 ± 1.8a	49.7 ± 0.4a	44.8 ± 7a
pH (pH unit)	8.6 ± 0a	8.6 ± 0a	8.5 ± 0a	8.41 ± 0a	8.6 ± 0a	8.5 ± 0a	8.5 ± 0a	8.4 ± 0a	8.5 ± 0a	8.5 ± 0a	8.3 ± 0a	8.4 ± 0a
Titratable acidity ($gCH_3COOH\ L^{1}$)	2.2 ± 0.3ba	2.8 ± 0b	1.8 ± 0a	2 ± 0.1a	1.8 ± 0.1c	1.4 ± 0b	1.1 ± 0a	1.9 ± 0.1c	1.5 ± 0.1a	1.48 ± 0.2a	1.1 ± 0a	1.6 ± 0.1a
Total alkalinity ($gCaCO_3\ L^{-1}$)	28.7 ± 0.1a	28.7 ± 0.1a	30.6 ± 0.5a	36.1 ± 2b	28.4 ± 0.2a	28 ± 0a	28.5 ± 0.9a	29.4 ± 0.2a	30.7 ± 0.8a	30.7 ± 1.6a	30.5 ± 1.8a	30.7 ± 0.4a
FOS/TAC	0.4 ± 0ba	0.5 ± 0b	0.3 ± 0a	0.3 ± 0a	0.3 ± 0b	0.2 ± 0ab	0.2 ± 0a	0.3 ± 0b	0.2 ± 0a	0.2 ± 0.1a	0.2 ± 0a	0.2 ± 0a
Ammonium-N ($gN\text{-}NH_4^+\ L^{-1}$)	3.2 ± 0a	3.2 ± 0.2a	3.2 ± 0.1a	3.2 ± 0a	2.6 ± 0a	2.9 ± 0.1a	2.7 ± 0a	2.4 ± 0.5a	3.2 ± 0a	3.4 ± 0.2a	3.5 ± 0.2a	3.6 ± 0.4a

[a] (Av. ± St. Dev., n = 3).
[b] Letters indicate statistical differences ($p \leq 0.05$) across the three runs for each parameter according to Tukey test.

2.5. 16S rRNA next-generation sequencing

DNA extraction was performed on all inocula and each digestate after each run. Samples (~40 ml) were pelleted at 13,000 rpm for 20 min. From each pellet, DNA was extracted using the DNeasy® PowerSoil® Kit (Qiagen, Germany) according to the manufacturer's instructions. DNA yield and purity were quantified on a Nanodrop 1000 spectrophotometer (Thermo Fisher Scientific) while quality was determined through gel electrophoresis 1 % (w/v) 1 × TAE agarose gels. DNA was stored at −80 °C until analysis.

The NGS was performed at Novogene Co. Ltd (Cambridge, UK). Sequencing targeted the V3 and V4 regions of the bacterial 16S rRNA gene using primers 341F (CCTAYGGGRBGCASCAG) and 806R (GGACTACNNGGGTATCTAAT) (Yu et al., 2005) and V4 region of the Archaeal 16S rRNA gene using primers U519F (CAGYMGCCRCGGKAAHACC) and 806R GGACTACNSGGGTMTCTAAT) (Porat et al., 2010). The generated DNA libraries were sequenced with an Illumina NovaSeq PE250, and the generated nucleotide sequences are available at the NCBI SRA repository (BioProject accession number: PRJNA1088852). The sequences resulting from the NGS were quality-checked through the FastQC software and analysed using DADA2 for R as per https://benjjneb.github.io/dada2/tutorial.html (Callahan et al., 2016). For the taxonomic assignment, the SILVA database v. 138.1 was used as a reference (McLaren and Callahan, 2021).

All microbial statistical analyses were performed on R studio (version 4.3.1) as by Clagnan et al. (2023) while MaAslin2 analyses were carried out as by https://huttenhower.sph.harvard.edu/maaslin/.

3. Result and discussion

3.1. Impact of acclimation on biogas production under mono- and co-digestion conditions

3.1.1. Cellulose

Cellulose was degraded similarly across the three runs and final biogas productions were close to theoretical production and previous research (Clagnan et al., 2023) indicating a functioning and reproducible system (Table 3).

3.1.2. OFMSW mono-digestion

Such as reported in Section 2.2, fresh inoculum taken directly from full scale plant before each run could be different therefore affecting AD processes (Table 1). To ensure data comparability across different runs,

Table 3
Biogas production and composition during the three anaerobic digestion runs.

	Parameter	Run 1 (29d) [a]	Run 2 (42d)	Run 3 (37d)
Cellulose	Biogas ($NLkgVS^{-1}$)	651[b] ± 34a[c]	593 ± 39a	576 ± 27a
	Biomethane ($NLkgVS^{-1}$)	413 ± 32a	397 ± 19a	391 ± 16a
	Biomethane (% v/v)	63.4 ± 1	66.9 ± 2	67.9 ± 5
OFMSW	Biogas ($NLkgVS^{-1}$)	597 ± 71a	719 ± 25b	730 ± 15b
	Biomethane ($NLkgVS^{-1}$)	341 ± 42a	517 ± 8b	535 ± 10b
	Biomethane (% v/v)	57.1 ± 2	71.9 ± 3	73.3 ± 2
PLA	Biogas ($NLkgVS^{-1}$)	330 ± 23a	831 ± 11c	710 ± 11b
	Biomethane ($NLkgVS^{-1}$)	227 ± 14a	466 ± 22c	362 ± 5b
	Biomethane (% v/v)	68.8 ± 2	56.1 ± 3	51.0 ± 1
PLA + OFMSW (Experimental)	Biogas ($NLkgVS^{-1}$)	488 ± 51a	827 ± 69b	749 ± 9b
	Biomethane ($NLkgVS^{-1}$)	326 ± 31a	485 ± 42b	430 ± 12b
	Biomethane (% v/v)	66.8 ± 2	58.7 ± 2	57.4 ± 2
PLA + OFMSW (Theoretical)	Biogas ($NLkgVS^{-1}$)	432 ± 31a	788 ± 16b	721 ± 11c
	Biomethane ($NLkgVS^{-1}$)	293 ± 18a	486 ± 13b	428 ± 5b

[a] The duration of the run (d) depended on the achievement of max cellulose biogas production, i.e. about 600 NL kg VS^{-1}.
[b] (Av. ± St. Dev.; n = 3).
[c] Letters indicate statistical differences ($p \leq 0.05$) across the three runs for each parameter according to Tukey test.

AD runs were carried on until the maximum cellulose (control) biogas production was achieved, i.e. 600 NL $kgVS^{-1}$ (Clagnan et al., 2023). Doing so AD length differed across runs (Table 3) and it was generally

lower for run 1 due to non-acclimation (Fig. 1).

The first run of OFMSW mono-digestion resulted in a production of 597 ± 71 NL $kgVS^{-1}$ (341 ± 42 $NLCH_4$ $kgVS^{-1}$). At the end of run 2 and 3 (i.e. after acclimatation), a significantly higher production of cumulative biogas was achieved (719 ± 25 NL $kgVS^{-1}$ and 517 ± 8 $NLCH_4$ $kgVS^{-1}$ for run 2; 730 ± 15 NL $kgVS^{-1}$ and 535 ± 10 $NLCH_4$ $kgVS^{-1}$ for run 3; i.e. +20 % and +22 % when compared to run 1; $p < 0.05$) (Table 3).

Differently from run 2 and 3, run 1 showed a curve of biogas production typical of inhibition and partial biogas production due to the toxic effects of VFAs and/or ammonium-N accumulation (Liu et al., 2016) (Fig. 1). In this study ammonium toxicity was excluded as its content was similar in runs where this pattern was not seen. On the other hand, the content of titratable acidity was higher ($p < 0.05$) in run 1 than the other runs, i.e 2.8 ± 0.0 g CH_3COOH L^{-1} for run 1 vs. 1.4 ± 0.0 and 1.48 ± 0.22 g CH_3COOH L^{-1}, for run 2 and 3 respectively (Table 2). Anaerobic digesters generally operate stably at VFA concentrations below 1–2 g L^{-1} (Angelidaki et al., 2005). In our study, run 1 showed a titratable acidity up to 2.8 ± 0.0 g CH_3COOH L^{-1}, which exceeded the common range indicated, leading to the partial inhibition of the methanation bacteria activity such as indicated by the reduced biomethane percentage, i.e. 57.1 ± 2 % of run 1 with respect runs 2 and 3 (i.e., 71.9 ± 3 and 73.3 ± 2 % respectively) (Table 3). Due to this partial inhibition occurred of run 1, the kinetic parameters for this run were not considered in the subsequent discussion ($R^2 < 0.967$).

The modified Gompertz model fit biogas production ($R^2 = 0.994$ and 0.982) (Table 4). Biogas production rate (R_{max}) and the lag phase remained constant between runs 2 and 3 (i.e. R_{max} of 39 and 38 NL $kgVS^{-1}d^{-1}$ and lag phases of 7 and 8 d) indicating that the microbial community was already optimized and adapted to efficiently degrade this substrate (Table 4).

Table 4
Kinetic analysis of biogas production during the three anaerobic digestions runs.

	Parameter	Run 1	Run 2	Run 3
OFMSW	B_0 (NL $kgVS^{-1}$)	755	755	755
	R_{max} (NL $kgVS^{-1}d^{-1}$)	20	39	38
	λ (d)	5	7	8
	R^2	0.891	0.994	0.982
	t_{90}[a] (d)	n.d.	31	32
PLA	B_0 (NL $kgVS^{-1}$)	840	840	840
	R_{max} (NL $kgVS^{-1}d^{-1}$)	27	47	39
	λ (d)	17	12	12
	R^2	0.997	0.996	0.985
	t_{90} (d)	54	33	38
PLA + OFMSW	B_0 (NL $kgVS^{-1}$)	806	806	806
	R_{max} (NL $kgVS^{-1}$ d^{-1})	42	58	51
	λ (d)	17	10	13
	R^2	0.967	0.994	0.985
	t_{90} (d)	40	27	32

[a] t_{90}: time required to get 90 % of the total producible biogas.

3.1.3. PLA mono-digestion

In run 1, the cumulative biogas produced from PLA in mono-digestion was of 330 ± 23 NL $kgVS^{-1}$227 ± 14 $NLCH_4$ $kgVS^{-1}$) (Table 3). This production is comparable to data previously reported by Clagnan et al. (2023) where PLA-based glasses mono-digested under similar AD conditions produced 395 ± 3 NL $kgVS^{-1}$ (233 $NLCH_4$ $kgVS^{-1}$). Moreover, Cucina et al. (2022) reported a slightly lower CH_4

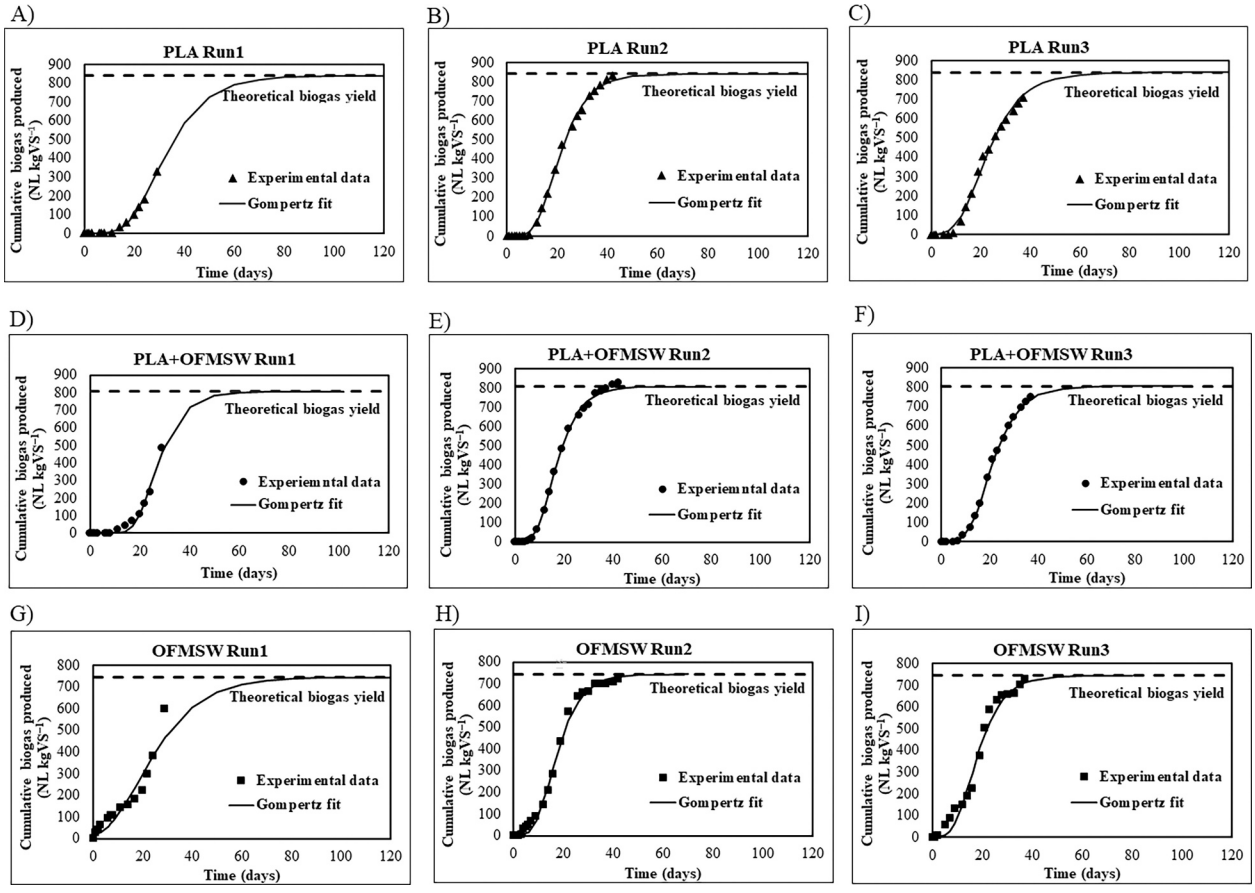

Fig. 1. Experimental and predicted biogas yields of each substrate based on Gompertz model across the three runs and treatments: PLA mono-digestion (A, B, C), co-digestion (PLA + OFMSW) (D, E, F), and OFMSW mono-digestion (G, H, I).

production achieving 215 ± 11 and 279 ± 20 NL $kgVS^{-1}$ after 60 days under similar conditions for PLA-based dishes and cutlery, respectively. Similarly, Vasmara and Marchetti (2016) obtained a slightly lower CH_4 yield of 282 NL $kgVS^{-1}$for PLA-based cups after 90 days under thermophilic condition. The differences in the degradation time observed between the studies could be explained by variations in the types or sources of the inoculum, as well as differences in the composition and physical properties of the PLA materials.

In run 2, biogas production increased to 831 ± 11 NL $kgVS^{-1}$ (466 ± 22 $NLCH_4$ $kgVS^{-1}$), i.e. +152 % compared to run 1 ($p < 0.05$). At the end of run 3, there was a decrease in biogas production to 710 ± 11 NL $kgVS^{-1}$ (362 ± 5 $NLCH_4$ $kgVS^{-1}$; i.e., −15 % compared to run 2; $p < 0.05$) although it was still higher than in run 1 (+115 %) (Table 3). The lower productivity of run 3 was associated to the shorter degradation time (37 days for run 3 instead of the 42 days of run 2). The ratio of biomethane to biogas, expressed as methane concentration (% v/v), was between 68.8 ± 2 and 51.0 ± 1 % (Table 3); while some variations were observed, the values remained within the range commonly reported for AD processes involving mixed substrates (50–70 %), indicating that methane production was consistently maintained throughout the experiment (Taramasso et al., 2024).

Again, the modified Gompertz model fitted biogas production (R^2 = 0.996 and 0.985 for run 2 and run 3, respectively) (Table 4). The PLA biogas production rate (R_{max}) showed an increase from 27 NL $kgVS^{-1}d^{-1}$ (lag phase of 17 d; R^2 = 0.997) in run 1 to 47 and 39 NL $kgVS^{-1}d^{-1}$ to run 2 and 3, respectively (lag phases of 12 d for both runs) (Table 4) (Fig. 1). The increase in the biogas production rate and the decrease in the lag phase indicated that microbial adaptation occurred within this treatment (Table 4).

For PLA mono-digestion, acclimation seems to be an efficient approach to improve the biodegradability of PLA. The degradation here obtained was similar to the degradability results obtained by PLA pretreatment in literature. For example, Zaborowska et al. (2023) reported that under thermophilic AD conditions, PLA-based cups pretreated by hydrothermal and alkaline treatments lead to a CH_4 production of 448 $NLCH_4$ $kgVS^{-1}$. Similarly, Jin et al. (2023) achieved a comparable CH_4 production (462.6 $NLCH_4$ $kgVS^{-1}$) through alkali pretreatment and thermophilic AD of ground PLA pellets. Alkaline and thermal pre-treatments are however associated with significant costs, energy consumption and environmental issues, affecting the overall sustainability of the process. On the other hand, microbial acclimatization is cost-effective and environmentally friendly and has the potential to be a strategy to promote the circular economy of bioplastics (Clagnan et al., 2023; Cucina et al., 2023).

3.1.4. PLA and OFMSW co-digestion

Co-digestion of PLA and OFMSW produced 488 ± 51 NL $kgVS^{-1}$(326 ± 31 $NLCH_4$ $kgVS^{-1}$) in run 1. At the end of run 2, a significant increase in biogas production was achieved (827 ± 69 NL $kgVS^{-1}$), i.e. + 69 % if compared to run 1 ($p < 0.05$). No significant difference was seen between runs 2 and 3 (Table 3). Biomethane concentration for PLA + FW co-digestion was consistently lower than that observed for OFMSW alone, indicating that CH_4 content depended by the substrate added, i.e. OFMSW containing fat produced biogas with more CH_4 (REF) than PLA, so that when PLA was added to OFMSW the CH_4 content decreased (see Table 3 run 2 and 3, run 1 was not considered to inhibition occurred).

Theoretical production, calculated starting form PLA and OFMSW mono-digestion, gave similar results to the experimental results indicating reproducibility and validating both the experimental work and data acquired. These results were a further indication that OFMSW and PLA degrade similarly in both mono- or co-digestion (Table 3).

The modified Gompertz kinetics showed an increase of the biogas production rate from 42 NL $kgVS^{-1}d^{-1}$ in run 1 (R^2 of 0.967) to a rate of 58 NL $kgVS^{-1}d^{-1}$ in run 2 (R^2 of 0.994). A reduction of the lag phase was also shown from 17 days to 10 d for run 1 and 2, respectively (Table 4) (Fig. 1). Run 3 (R^2 of 0.985) showed a slightly reduction of the R_{max} when compared to run 2 (51 NL $kgVS^{-1}d^{-1}$) and a lag phase of 13 days (Table 4). These data indicated that the biogas production rate increased with acclimatation. It can be assumed that for run 1 the contribution to biogas production came above all from OFMSW degradation as microbial adaptation was not required for an efficient degradation (see Section 3.1.2) and less from PLA degradation. In run 2 and run 3, the adaptation of the microbial population to PLA, started to contribute to biogas production reducing lag phase. Interesting the lag phase trend observed for PLA + OFMSW was the same of PLA mono-digestion. These results seem to confirm that microbial adaptation is needed to maximize PLA degradation.

3.2. Prokaryotic communities' characterization

The composition and dynamics of the bacterial communities of all treatments (i.e., inoculum, negative control, cellulose, OFMSW, PLA, and PLA + OFMSW) were investigated for the three batch runs performed (i.e., run 1, run 2, and run 3) through a 16S rRNA sequencing analysis with a double couple of primers one dedicated to Bacteria and one to Archaea.

3.2.1. Bacteria

Bacterial NGS analysis produced between 151,934 and 219,794 input reads while between 118,915 and 179,089 reads after DADA2 assignment (Fig. S2).

When looking at the phyla composition, all samples showed a similar composition. Similarly to Clagnan et al. (2023), main phyla (above 2 %) across most samples were Firmicutes, Cloacimonadota, Bacteroidota and Synergistota with Proteobacteria characterizing the run 3 of all treatments (Fig. S3). Proteobacteria, Bacteroidota, Firmicutes, and Synergistota have been shown to enhance substrate (often lignocellulosic) degradation (i.e. hydrolysis, acidogenesis and acetogenesis) (Li and Huang, 2024). Firmicutes and Bacteroidetes have been linked to process performance and its parameters such as organic loading rate, volatile fatty acids concentration, and methane production (Chen et al., 2016), while Cloacimonadota to mutual metabolic interactions with methanogens (Feng et al., 2023).

When looking at the structure at genus level (abundance > 5 %), the inoculum was characterized by *Fastidiosipila* at both run 1 (14 %) and run 2 (12 %), a proteolytic and VFAs-producing bacteria (Wang et al., 2023), with the addition of the thermotolerant organic matter degrader *Sinibacillus* (10 %) at run 2 (Zhen et al., 2021), while run 3 showed the presence of the denitrifier *Pusillimonas* (10 %) (Fang et al., 2023), *Sinibacillus* (7 %), and the carbohydrates fermenter *Lentimicrobium* (5 %) (Li et al., 2022) (Fig. 2).

The negative controls were characterized by a similar genera (>5%) composition of proteolytic bacteria, denitrifiers and starch, casein, and tributyrin hydrolysers with high NH_3 tolerance (Perman et al., 2022) (Fig. 2).

The positive control (cellulose) showed again a similar composition with the addition of an enrichment in *Halocella* increasing from run 2 (14 %) to run 3 (27 %) (Fig. 2). *Halocella* are hemicellulose and starch degraders whose growth seems to be impaired by the presence of PLA (Zheng et al., 2023; Wahid and Horn, 2021) and it was retrieved for the same treatment also in Clagnan et al. (2023).

The OFMSW treatment was characterized by *Fastidiosipila* (12 %) and *Halocella* (6 %) at run 1. At run 2 *Fastidiosipila* (8 %) was followed by *Caldicoprobacter* (7 %), another glucose-based acidogen (Xiao et al., 2024), with a combination of *Lentimicrobium* (7 %), *Halocella* (5 %) and *Caldicoprobacter* (5 %), at run 3 (Fig. 2). The PLA treatment was characterized again by *Fastidiosipila* (12 %) with the addition of *Tepidanaerobacter* (9 %) at run1. Run 2 showed again the presence of *Fastidiosipila* (7 %) and *Acetomicrobium* (6 %) with an increase *Tepidanaerobacter* (14 %). *Tepidanaerobacter* (23 %) showed a further increase in run 3 accompanied by *Lentimicrobium* (8 %) (Fig. 2). Similarly to *Lentimicrobium*, *Tepidanaerobacter, a* lactate-degrading bacterium, is

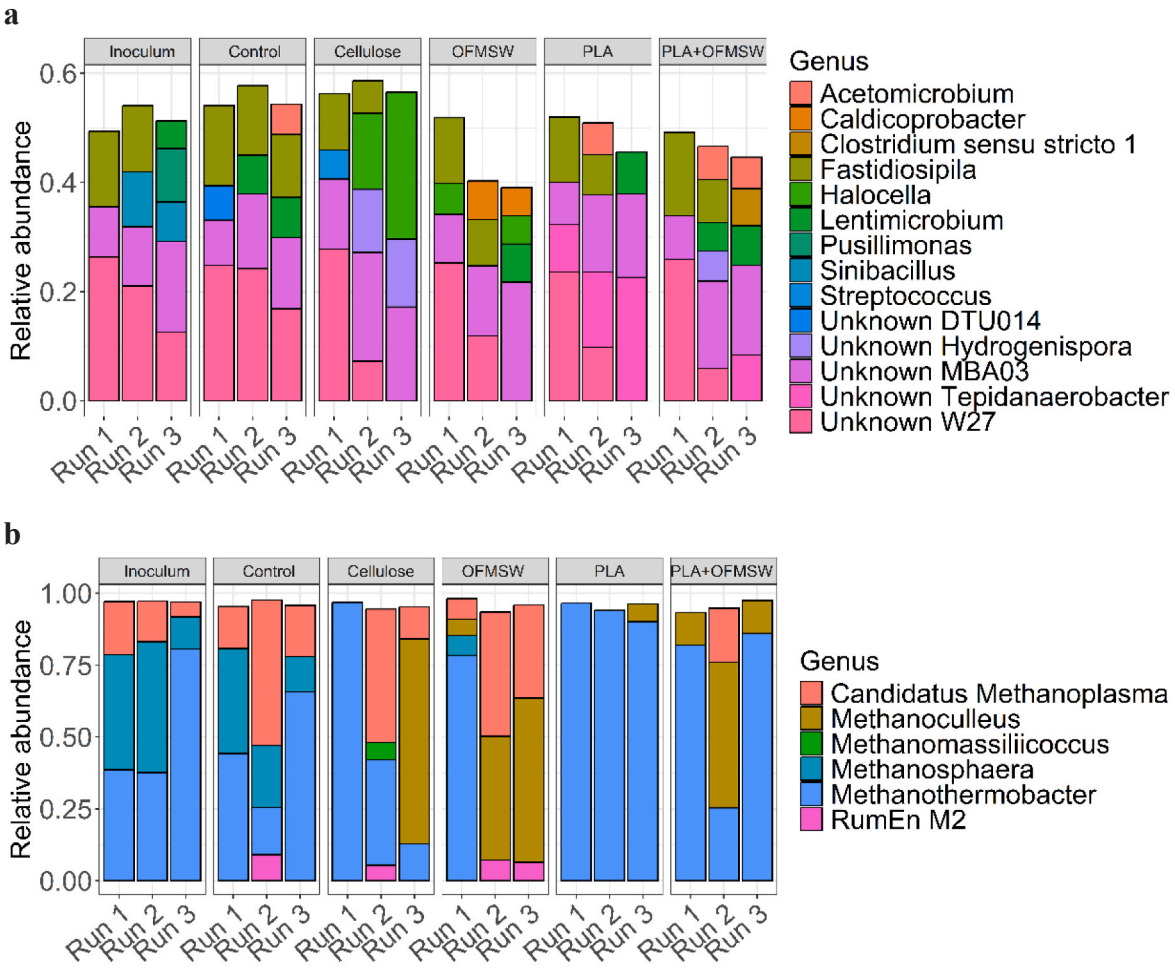

Fig. 2. Bacterial (a) and archaeal (b) communities' composition at genus level with a >5 % cut-off (Av., n = 2).

positively linked to propionic and butyric acid accumulation (Xiao et al., 2024) and has been shown to positively correlate also with the increasing methane production from PLA in the thermophilic reactors (Cazaudehore et al., 2022b; Clagnan et al., 2023). Its increase in abundance over time can be seen as an indication of acclimation of the community.

Generally, co-digestion of PLA and OFMSW showed a mixed composition of genera (>5%) between PLA and OFMSW mono-

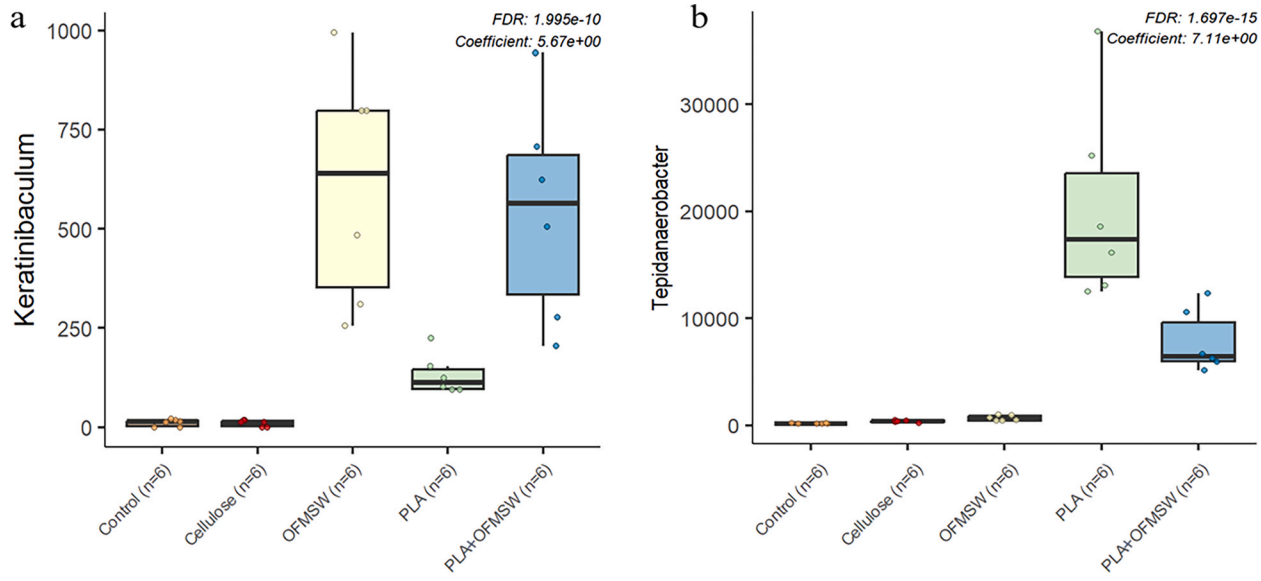

Fig. 3. Selection of the most enriched genera across treatments from MaAsLin2 analysis.

digestion. Run 1 showed the presence of *Fastidiosipila* (15 %), while at run 2 *Fastidiosipila* (8 %) was followed by *Acetomicrobium* (6 %) and *Lentimicrobium* (5 %). At run 3, *Acetomicrobium* (6 %) and *Lentimicrobium* (7 %) were followed by *Tepidanaerobacter* (8 %) and the H_2-producing bacteria *Clostridium* sensu stricto 1 (7 %) (Fig. 2).

Across most samples, genera belonging to the family of W27 and the order of MBA03 were further encountered. They are frequently observed in cellulose-based biogas reactors, and MBA03 has been found to be a potential syntrophic acetate-oxidizer which follows similar trends to hydrogenotrophic methanogens (Perman et al., 2022).

When looking at the most enriched genera across all treatments, a significant enrichment in *Tepidanaerobacter* can be further confirmed for PLA and PLA + OFMSW. Conversely, OFMSW and PLA + OFMSW showed a further enrichment in the proteolytic bacterium *Keratinibaculum* (Fig. 3). The increase in protein and starch degraders is most likely driven by a dual cause, the substrate high in starch and protein (due also to the increasing biomass from digestate recycling) and secondly as protein degraders are directly contributing to PLA degradation as multiple bacterial proteases have been proven to be enzymatically active for PLA hydrolysis (e.g. the hydrolytic activity of Bacteroidales protease) (Zhu et al., 2023).

3.2.2. Archaea

Archaeal NGS produced between 184,132 and 219,745 input reads while between 108,131 and 187,393 reads after DADA2 assignment (Fig. S2).

Archaeal phyla composition (above 2 %), included three main phyla, all containing methanogens: (i) Euryarchaeota, generally hydrogenotrophic, acetoclastic, methylotrophic, or H_2-dependent methylotrophic (Kumar et al., 2021), (ii) Halobacterota, mainly aerobic halophiles that possibly evolved from anaerobic methanogens (Martijn et al., 2020), and (iii) Thermoplasmatota that thrives under energy limitation thanks to a metabolic potentials for the degradation of aromatic and halogenated organic compound and alkane utilization (Zheng et al., 2022) (Fig. S3).

Considering the most abundant archaeal genera (above 5 %), the inocula and the negative controls showed a similar composition with the presence of mainly three genera: a candidatus *Methanoplasma*, and two hydrogenotrophic methanogens *Methanosphaera* (Ros et al., 2017) and *Methanothermobacter* (Tian et al., 2015) (Fig. 2). Candidatus *Methanoplasma* is an understudied methanogen which has been found in the AD processes that is however correlated to low methane production (Vendruscolo et al., 2020). On the other hand, *Methanothermobacter* has been found to outcompete other methanogens thanks to its syntrophic relationship with fatty acid-oxidizers (Yan et al., 2020).

The positive control (cellulose) showed *Methanothermobacter* as main genera at run 1 (97 %), which was retrieved also at run 2 (37 %) together with candidatus *Methanoplasma* (46 %). In run 3, the community switched to *Methanoculleus* (71 %), a genus that has been found in literature to positively correlate with high ammonia levels and high methane production (Ziganshin et al., 2016) (Fig. 2).

Similarly to cellulose, OFMSW showed *Methanothermobacter* (78 %) at run 1 with a small presence of candidatus *Methanoplasma* (7 %), *Methanoculleus* (6 %) and *Methanosphaera* (7 %) while both run 2 and 3 were characterized by a higher abundance of candidatus *Methanoplasma* (43 % and 32 %, respectively) and *Methanoculleus* (43 % and 57 %, respectively), with traces of *RumEn M2* (7 % and 6 %, respectively) (Fig. 2).

PLA was characterized across all runs by *Methanothermobacter* (90–97 %) with only a small abundance of *Methanoculleus* at run 3 (6 %) (Fig. 2).

PLA + OFMSW showed, both at run 1 and 3 a high abundance of *Methanothermobacter* (82 % and 86 %, respectively) together with *Methanoculleus* (both 11 %). Run 2 showed a higher abundance of *Methanoculleus* (51 %) than *Methanothermobacter* (25 %) with also the presence of candidatus *Methanoplasma* (19 %) (Fig. 2).

Ammonia released from AD usually leads to suboptimal conditions with methanogens being the most vulnerable to high NH_4^+-N concentrations (Yan et al., 2020). High NH_4^+-N suppressed acetoclastic methanogenesis to the advantage of hydrogenotrophic methanogens, as seen in this study. A genomic analysis of hydrogenotrophic methanogens has found that Methanomassiliicoccales and *Methanothermobacter* carry out methanogenesis from methanol and formate (respectively) and H_2/CO_2 which is highly exergonic and might lead to a higher ammonia tolerance than *Methanoculleus* from acetate and H_2/CO_2 (Yan et al., 2020). However, a more recent study has shown how *Methanoculleus* is consistently enriched under inhibitory levels of NH_4^+-N pushing CH_4 productions over other genera such as *Methanothermobacter* (Finn et al., 2023). The same study highlighted how the adaptation of a community leads to a higher methanogenesis under suboptimal NH_4^+-N concentrations and how a successful and robust system is the results not of specific taxa but of the constant interaction and redundances between tolerant methanogens and other tolerant taxa (i.e. broad-scale tolerance) (Finn et al., 2023). In this context, when looking at CH_4 production, PLA showed a trend of lower diversity among the three treatments (OFMSW, PLA + OFMSW and PLA) (Fig. S4) and a lower abundance of *Methanoculleus,* which might have led to the trend of lower production especially in run 3.

3.3. PLA degradation vs. Microbial acclimatation

These results appear of great interest considering the upscale potential to a full-scale plant treating OFMSW wastes containing bioplastics. In particular, full scale anaerobic digestion must be able to (i) completely degrade PLA therefore avoiding or limiting the content of PLA in the final digestate and (ii) maximize biogas production to which PLA is contributing (Abraham et al., 2021; Cazaudehore et al., 2022a).

Literature reported that acceptable AD performance in continuous stirred-tank reactors (CSTR) allows the achievement 90 % of producible biogas (t_{90}) from OFMSW at a HRT of 30 days (Schievano et al., 2011). In this work, kinetics analyses performed using experimental data indicated that microbial adaptation allowed the reduction of the t_{90} from 54 and 40 days to 33–38 and 27–32 days, for PLA mono- and co-digestion respectively (Table 4). These enhanced (t_{90}) values obtained from PLA mono- and co-digestion are in line with the HRT typically applied within the real-scale OFMSW treating plant cited above.

These results showed that microbial acclimation is an efficient strategy to achieve a faster PLA biodegradation characterised by a shorter lag phase and an increase of the biogas production rate, indicating the potential to apply this concept to CSTRs at full-scale leading to a more sustainable bioplastic waste management in the context of circular economy. This study is of interest when considering future upscaling to full-scale. Microbial acclimation can be applied through two main approaches: pre-acclimation of the inoculum to the target substrate prior to reactor start-up and gradual in situ acclimation during continuous digestion by gradually increasing the organic loading rate. While no full-scale CSTR studies have yet implemented these strategies for bioplastics, their effectiveness has been demonstrated for other complex substrates. For instance, Wojcieszak et al. (2017) showed that both pre-acclimation and in situ acclimation enhanced biogas production and process stability during maize silage digestion, while Gonçalves et al. (2012) demonstrated similar improvements using pre-acclimated inoculum with olive mill wastewater. These findings strongly support the potential applicability of microbial acclimation strategies to the industrial-scale AD of bioplastics. Overall, microbial acclimation is promising and effective strategy for enhancing biogas production from PLA, both in mono-digestion and co-digestion systems. Furthermore, its application in the co-digestion of bioplastics with OFMSW will further avoid the need for de-packaging, and relative loss of OFMSW, thus increasing process profitability.

4. Conclusions

Microbial acclimation was a strong enhancer of PLA biodegradation and biogas production through thermophilic AD both alone and in co-digestion with OFMSW. After microbial acclimation, biogas productions and the kinetic rate of both PLA mono-digestion and co-digestion were enhanced and linked to an enrichment in PLA degrading bacteria such as *Tepidanaerobacter*; these were also characterized by a high abundance of hydrogenotrophic Archaea member such as Methanothermobacter and Metanoculleus. The time required to degrade at least 90 % of PLA was reduced after microbial acclimatation leading to a degradation time that is comparable with HRTs commonly used in CSTRs of full-scale AD plants. These results suggest that microbial acclimation is a useful strategy to improve PLA degradation efficiency especially in co-digestion with OFMSW therefore the use of this technique might lead, after further targeted research, to its use in AD full-scale plant improving PLA waste management.

CRediT authorship contribution statement

Hager Galal Elsayed Elboghdady: Writing – review & editing, Writing – original draft, Visualization, Validation, Methodology, Investigation, Formal analysis, Data curation, Conceptualization. **Elisa Clagnan:** Writing – review & editing, Writing – original draft, Visualization, Validation, Supervision, Methodology, Formal analysis, Data curation, Conceptualization. **Veronica De Franceschi:** Validation, Investigation, Data curation. **Mirko Cucina:** Writing – review & editing, Validation, Methodology, Data curation. **Marta Dell'Orto:** Writing – review & editing, Methodology, Investigation. **Patrizia De Nisi:** Writing – review & editing. **Andrea Goglio:** Methodology. **Fabrizio Adani:** Writing – review & editing, Supervision, Resources, Funding acquisition, Conceptualization.

Declaration of competing interest

The authors declare that they have no known competing financial interests or personal relationships that could have appeared to influence the work reported in this paper.

Acknowledgements

This work was funded by Gruppo RICICLA, Department of Agricultural and Environmental Sciences - Production, Territory, Agroenergy (DiSAA), University of Milan. Fund: 34433_CTE_NAZPU20FADAN_01.

Appendix A. Supplementary data

Supplementary data to this article can be found online at https://doi.org/10.1016/j.wasman.2025.114895.

Data availability

Data will be made available on request.

References

Abraham, A., Park, H., Choi, O., Sang, B.I., 2021. Anaerobic co-digestion of bioplastics as a sustainable mode of waste management with improved energy production – A review. *Bioresour. Technol.* 322, 124537. https://doi.org/10.1016/J.BIORTECH.2020.124537.

Angelidaki, I., Boe, K., Ellegaard, L., 2005. Effect of operating conditions and reactor configuration on efficiency of full-scale biogas plants. *Water Sci. Technol.* 52 (1–2), 189–194. https://doi.org/10.2166/wst.2005.0516.

Bernat, K., Kulikowska, D., Wojnowska-Baryła, I., Zaborowska, M., Pasieczna-Patkowska, S., 2021. Thermophilic and mesophilic biogas production from PLA-based materials: Possibilities and limitations. *Waste Manag.* 119, 295–305. https://doi.org/10.1016/J.WASMAN.2020.10.006.

Buswell, A.M., Mueller, H.F., 1952. Mechanism of Methane Fermentation. *Ind. Eng. Chem.* 44 (3), 550–552. https://doi.org/10.1021/IE50507A033.

Callahan, B.J., McMurdie, P.J., Rosen, M.J., Han, A.W., Johnson, A.J.A., Holmes, S.P., 2016. DADA2: High-resolution sample inference from Illumina amplicon data. Nature Methods 13 (7), 581–583. https://doi.org/10.1038/nmeth.3869.

Cazaudehore, G., Guyoneaud, R., Evon, P., Martin-Closas, L., Pelacho, A.M., Raynaud, C., Monlau, F., 2022a. Can anaerobic digestion be a suitable end-of-life scenario for biodegradable plastics? A critical review of the current situation, hurdles, and challenges. *Biotechnol. Adv.* 56, 107916. https://doi.org/10.1016/J.BIOTECHADV.2022.107916.

Cazaudehore, G., Guyoneaud, R., Lallement, A., Gassie, C., Monlau, F., 2022b. Biochemical methane potential and active microbial communities during anaerobic digestion of biodegradable plastics at different inoculum-substrate ratios. *J. Environ. Manage.* 324, 116369. https://doi.org/10.1016/J.JENVMAN.2022.116369.

Cazaudehore, G., Guyoneaud, R., Lallement, A., Souquet, P., Gassie, C., Sambusiti, C., Grassl, B., Jiménez-Lamana, J., Cauzzi, P., Monlau, F., 2023a. Simulation of biowastes and biodegradable plastics co-digestion in semi-continuous reactors: Performances and agronomic evaluation. *Bioresour. Technol.* 369, 128313. https://doi.org/10.1016/J.BIORTECH.2022.128313.

Cazaudehore, G., Guyoneaud, R., Vasmara, C., Greuet, P., Gastaldi, E., Marchetti, R., Leonardi, F., Turon, R., Monlau, F., 2022c. Impact of mechanical and thermo-chemical pretreatments to enhance anaerobic digestion of poly(lactic acid). *Chemosphere* 297, 133986. https://doi.org/10.1016/J.CHEMOSPHERE.2022.133986.

Cazaudehore, G., Monlau, F., Gassie, C., Lallement, A., Guyoneaud, R., 2021. Methane production and active microbial communities during anaerobic digestion of three commercial biodegradable coffee capsules under mesophilic and thermophilic conditions. *Sci. Total Environ.* 784, 146972. https://doi.org/10.1016/J.SCITOTENV.2021.146972.

Cazaudehore, G., Monlau, F., Gassie, C., Lallement, A., Guyoneaud, R., 2023b. Active microbial communities during biodegradation of biodegradable plastics by mesophilic and thermophilic anaerobic digestion. *J. Hazard. Mater.* 443, 130208. https://doi.org/10.1016/J.JHAZMAT.2022.130208.

Chen, S., Cheng, H., Wyckoff, K.N., He, Q., 2016. Linkages of Firmicutes and Bacteroidetes populations to methanogenic process performance. *J. Ind. Microbiol. Biotechnol.* 43 (6), 771–781. https://doi.org/10.1007/S10295-016-1760-8.

Chiappero, M., Berruti, F., Mašek, O., Fiore, S., 2021. Analysis of the influence of activated biochar properties on methane production from anaerobic digestion of waste activated sludge. *Biomass Bioenergy* 150, 106129. https://doi.org/10.1016/J.BIOMBIOE.2021.106129.

Chickering, G.W., Krause, M.J., Townsend, T.G., 2018. Determination of as-discarded methane potential in residential and commercial municipal solid waste. *Waste Manag.* 76, 82–89. https://doi.org/10.1016/j.wasman.2018.03.017.

Clagnan, E., Cucina, M., Vilas Sajgule, R., De Nisi, P., Adani, F., 2023. Microbial community acclimatization enhances bioplastics biodegradation and biogas production under thermophilic anaerobic digestion. *Bioresour. Technol.* 390, 129889. https://doi.org/10.1016/J.BIORTECH.2023.129889.

Cucina, M., De Nisi, P., Adani, F., 2023. Thermo-alkaline pre-treatment operated by digestate improved biomethane production of bioplastic. *Bioresour. Technol. Rep.* 21, 101374. https://doi.org/10.1016/J.BITEB.2023.101374.

Cucina, M., de Nisi, P., Tambone, F., Adani, F., 2021a. The role of waste management in reducing bioplastics' leakage into the environment: A review. *Bioresour. Technol.* 337, 125459. https://doi.org/10.1016/J.BIORTECH.2021.125459.

Cucina, M., De Nisi, P., Trombino, L., Tambone, F., Adani, F., 2021b. Degradation of bioplastics in organic waste by mesophilic anaerobic digestion, composting and soil incubation. *Waste Manag.* 134, 67–77. https://doi.org/10.1016/J.WASMAN.2021.08.016.

Cucina, M., Soggia, G., De Nisi, P., Giordano, A., Adani, F., 2022. Assessing the anaerobic degradability and the potential recovery of biomethane from different biodegradable bioplastics in a full-scale approach. *Bioresour. Technol.* 354, 127224. https://doi.org/10.1016/J.BIORTECH.2022.127224.

de Lemos Chernicharo, C.A., 2007. Anaerobic Reactors, 9781780402116-9781780402116 *Water Intell. Online* 6. https://doi.org/10.2166/9781780402116.

Di Maria, F., Sordi, A., Cirulli, G., Gigliotti, G., Massaccesi, L., Cucina, M., 2014. Co-treatment of fruit and vegetable waste in sludge digesters. An analysis of the relationship among bio-methane generation, process stability and digestate phytotoxicity. *Waste Manag.* 34 (9), 1603–1608. https://doi.org/10.1016/J.WASMAN.2014.05.017.

El-Mashad, H.M., Zhang, R., Greene, J.P., 2012. Anaerobic biodegradability of selected biodegradable plastics and biobased products. *J. Environ. Sci. Eng. A* 1 (1A).

European Bioplastics, 2024. Bioplastics market data 2024. https://docs.european-bioplastics.org/publications/market_data/2024/EUBP_Market_Data_Report_2024.pdf . Accessed 24th Jan 2024.

Fang, T., Wang, T., Zhao, M., Bai, L., Deng, Y., Ruan, W., 2023. Food waste digestate composting enhancement by sodium polyacrylate addition: Effects on nitrogen transformation processes and bacterial community dynamics. *J. Environ. Manage.* 325, 116531. https://doi.org/10.1016/J.JENVMAN.2022.116531.

Feng, L., Liu, C., Song, J., 2023. Effect of Mixed Antibiotics on Methane Production and Microbial Diversity during Anaerobic Digestion of Chicken Manure. *J. Environ. Eng.* 150 (2), 04023101. https://doi.org/10.1061/JOEEDU.EEENG-7390.

Finn, D.R., Rohe, L., Krause, S., Guliyev, J., Loewen, A., Tebbe, C.C., 2023. Methanogenesis in biogas reactors under inhibitory ammonia concentration requires community-wide tolerance. *Appl. Microbiol. Biotechnol.* 107 (21), 6717–6730. https://doi.org/10.1007/S00253-023-12752-5/FIGURES/6.

García-Depraect, O., Lebrero, R., Martínez-Mendoza, L.J., Rodriguez-Vega, S., Aragão Börner, R., Börner, T., Muñoz, R., 2023. Enhancement of biogas production rate from bioplastics by alkaline pretreatment. *Waste Manag.* 164, 154–161. https://doi.org/10.1016/J.WASMAN.2023.04.009.

Gonçalves, M.R., Costa, J.C., Marques, I.P., Alves, M.M., 2011. Inoculum acclimation to oleate promotes the conversion of olive mill wastewater to methane. *Energy* 36 (4), 2138–2141. https://doi.org/10.1016/J.ENERGY.2010.04.042.

ISO 14855-2:2018 - Determination of the ultimate aerobic biodegradability of plastic materials under controlled composting conditions — Method by analysis of evolved carbon dioxide — Part 2: Gravimetric measurement of carbon dioxide evolved in a laboratory-scale test. Retrieved May 22, 2023, from https://www.iso.org/standard/72046.html.

Jin, Y., Cai, F., Song, C., Liu, G., Chen, C., 2022. Degradation of biodegradable plastics by anaerobic digestion: Morphological, micro-structural changes and microbial community dynamics. *Sci. Total Environ.* 834, 155167. https://doi.org/10.1016/J.SCITOTENV.2022.155167.

Jin, Y., Sun, X., Song, C., Cai, F., Liu, G., Chen, C., 2023. Understanding the mechanism of enhanced anaerobic biodegradation of biodegradable plastics after alkaline pretreatment. *Sci. Total Environ.* 873, 162324. https://doi.org/10.1016/J.SCITOTENV.2023.162324.

Kumar, A., Samadder, S.R., 2020. Performance evaluation of anaerobic digestion technology for energy recovery from organic fraction of municipal solid waste: A review. *Energy* 197, 117253. https://doi.org/10.1016/J.ENERGY.2020.117253.

Kumar, V., Nabaterega, R., Khoei, S., Eskicioglu, C., 2021. Insight into interactions between syntrophic bacteria and archaea in anaerobic digestion amended with conductive materials. *Renew. Sustain. Energy Rev.* 144, 110965. https://doi.org/10.1016/J.RSER.2021.110965.

Li, J., Huang, C., 2024. Anaerobic co-digestion of corn straw, sewage sludge and fresh leachate: Focusing on synergistic/antagonistic effects and microbial mechanisms. *Bioresour. Technol.* 395, 130414. https://doi.org/10.1016/J.BIORTECH.2024.130414.

Li, M.T., Rao, L., Wang, L., Gou, M., Sun, Z.Y., Xia, Z.Y., Song, W.F., Tang, Y.Q., 2022. Bioaugmentation with syntrophic volatile fatty acids-oxidizing consortia to alleviate the ammonia inhibition in continuously anaerobic digestion of municipal sludge. *Chemosphere* 288, 132389. https://doi.org/10.1016/J.CHEMOSPHERE.2021.132389.

Liu, C., Li, H., Zhang, Y., Liu, C., 2016. Improve biogas production from low-organic-content sludge through high-solids anaerobic co-digestion with food waste. Bioresour. Technol. 219, 252–260. https://doi.org/10.1016/j.biortech.2016.07.130.

Lu, B., Jiang, C., Chen, Z., Li, A., Wang, W., Zhang, S., Luo, G., 2022. Fate of polylactic acid microplastics during anaerobic digestion of kitchen waste: Insights on property changes, released dissolved organic matters, and biofilm formation. *Sci. Total Environ.* 834, 155108. https://doi.org/10.1016/J.SCITOTENV.2022.155108.

Martijn, J., Schön, M.E., Lind, A.E., Vosseberg, J., Williams, T.A., Spang, A., Ettema, T.J.G., 2020. Hikarchaeia demonstrate an intermediate stage in the methanogen-to-halophile transition. Nat. Commun. 11 (1), 1–14. https://doi.org/10.1038/s41467-020-19200-2.

Mu, L., Zhang, L., Ma, J., Zhu, K., Chen, C., Li, A., 2021. Enhanced biomethanization of waste polylactic acid plastic by mild hydrothermal pretreatment: Taguchi orthogonal optimization and kinetics modeling. *Waste Manag.* 126, 585–596. https://doi.org/10.1016/J.WASMAN.2021.03.044.

Peng, W., Wang, Z., Shu, Y., Lü, F., Zhang, H., Shao, L., He, P., 2022. Fate of a biobased polymer via high-solid anaerobic co-digestion with food waste and following aerobic treatment: Insights on changes of polymer physicochemical properties and the role of microbial and fungal communities. *Bioresour. Technol.* 343, 126079. https://doi.org/10.1016/J.BIORTECH.2021.126079.

Perman, E., Schnürer, A., Björn, A., Moestedt, J., 2022. Serial anaerobic digestion improves protein degradation and biogas production from mixed food waste. *Biomass Bioenergy* 161, 106478. https://doi.org/10.1016/J.BIOMBIOE.2022.106478.

Porat, I., Vishnivetskaya, T.A., Mosher, J.J., Brandt, C.C., Yang, Z.K., Brooks, S.C., Liang, L., Drake, M.M., Podar, M., Brown, S.D., Palumbo, A.V., 2010. Characterization of archaeal community in contaminated and uncontaminated surface stream sediments. *Microb. Ecol.* 60 (4), 784–795. https://doi.org/10.1007/s00248-010-9734-2.

Ros, M., de Souza Oliveira Filho, J., Perez Murcia, M.D., Bustamante, M.A., Moral, R., Coll, M.D., Lopez Santisima-Trinidad, A.B., Pascual, J.A., 2017. Mesophilic anaerobic digestion of pig slurry and fruit and vegetable waste: Dissection of the microbial community structure. J. Clean. Prod. 156, 757–765. https://doi.org/10.1016/J.JCLEPRO.2017.04.110.

Samoraj, M., Mironiuk, M., Izydorczyk, G., Witek-Krowiak, A., Szopa, D., Moustakas, K., Chojnacka, K., 2022. The challenges and perspectives for anaerobic digestion of animal waste and fertilizer application of the digestate. *Chemosphere* 295, 133799. https://doi.org/10.1016/J.CHEMOSPHERE.2022.133799.

Schievano, A., D'Imporzano, G., Orzi, V., Adani, F., 2011. On-field study of anaerobic digestion full-scale plants (Part II): New approaches in monitoring and evaluating process efficiency. *Bioresour. Technol.* 102 (19), 8814–8819. https://doi.org/10.1016/J.BIORTECH.2011.07.012.

Schievano, A., Scaglia, B., D'Imporzano, G., Malagutti, L., Gozzi, A., Adani, F., 2009. Prediction of biogas potentials using quick laboratory analyses: Upgrading previous models for application to heterogeneous organic matrices. *Bioresour. Technol.* 100 (23), 5777–5782. https://doi.org/10.1016/j.biortech.2009.05.075.

McLaren, M. R., Callahan, B. J., 2021. *Silva 138.1 prokaryotic SSU taxonomic training data formatted for DADA2.* (n.d.). Doi: 10.5281/ZENODO.4587955.

Tambone, F., Scaglia, B., D'Imporzano, G., Schievano, A., Orzi, V., Salati, S., Adani, F., 2010. Assessing amendment and fertilizing properties of digestates from anaerobic digestion through a comparative study with digested sludge and compost. *Chemosphere* 81 (5), 577–583. https://doi.org/10.1016/J.CHEMOSPHERE.2010.08.034.

Taneepanichskul, N., Purkiss, D., Miodownik, M., 2022. A review of sorting and separating technologies suitable for compostable and biodegradable plastic packaging. *Front. Sust.* 3, 901885. https://doi.org/10.3389/frsus.2022.901885.

Taramasso, M.A., Motaghi, M., Casasso, A., 2024. A techno-economic feasibility analysis of solutions to cover the thermal and electrical demands of anaerobic digesters. *Renew. Energy* 236, 121485. https://doi.org/10.1016/j.renene.2024.121485.

Tian, Z., Zhang, Y., Li, Y., Chi, Y., Yang, M., 2015. Rapid establishment of thermophilic anaerobic microbial community during the one-step startup of thermophilic anaerobic digestion from a mesophilic digester. *Water Res.* 69, 9–19. https://doi.org/10.1016/J.WATRES.2014.11.001.

Vendruscolo, E.C.G., Mesa, D., Rissi, D.V., Meyer, B.H., de Oliveira Pedrosa, F., de Souza, E.M., Cruz, L.M., 2020. Microbial communities network analysis of anaerobic reactors fed with bovine and swine slurry. *Sci. Total Environ.* 742, 140314. https://doi.org/10.1016/J.SCITOTENV.2020.140314.

Wahid, R., Horn, S.J., 2021. Impact of operational conditions on methane yield and microbial community composition during biological methanation in in situ and hybrid reactor systems. *Biotechnol. Biofuels* 14 (1), 1–15. https://doi.org/10.1186/s13068-021-02019-4.

Wang, P., Li, X., Li, Y., Su, Y., Wu, D., Xie, B., 2023. Enhanced anaerobic digestion performance of food waste by zero-valent iron and iron oxides nanoparticles: Comparative analyses of microbial community and metabolism. *Bioresour. Technol.* 371, 128633. https://doi.org/10.1016/J.BIORTECH.2023.128633.

Xiao, M., Wang, N., Zhang, S., Hu, P., Xie, B., Shi, J., Liu, L., 2024. Synergistic bioaugmentation with Clostridium thermopalmarium and Caldibacillus thermoamylovorans improved methane production from thermophilic anaerobic digestion of food waste. *Chem. Eng. J.* 480, 148372. https://doi.org/10.1016/J.CEJ.2023.148372.

Yan, M., Treu, L., Zhu, X., Tian, H., Basile, A., Fotidis, I.A., Campanaro, S., Angelidaki, I., 2020. Insights into ammonia adaptation and methanogenic precursor oxidation by genome-centric analysis. *Environ. Sci. Tech.* 54 (19), 12568–12582. https://doi.org/10.1021/acs.est.0c01945.

Yu, Y., Lee, C., Kim, J., Hwang, S., 2005. Group-specific primer and probe sets to detect methanogenic communities using quantitative real-time polymerase chain reaction. *Biotechnol. Bioeng.* 89 (6), 670–679. https://doi.org/10.1002/BIT.20347.

Zaborowska, M., Bernat, K., Pszczółkowski, B., Cydzik-Kwiatkowska, A., Kulikowska, D., Wojnowska-Baryła, I., 2023. Multi-faceted analysis of thermophilic anaerobic biodegradation of poly(lactic acid)-based material. *Waste Manag.* 155, 40–52. https://doi.org/10.1016/J.WASMAN.2022.10.031.

Zhen, F., Luo, X., Xing, T., Sun, Y., Kong, X., Li, W., 2021. Performance evaluation and microbial community analysis of microaerobic pretreatment on thermophilic dry anaerobic digestion. *Biochem. Eng. J.* 167, 107873. https://doi.org/10.1016/J.BEJ.2020.107873.

Zheng, P.-F., Wei, Z., Zhou, Y., Li, Q., Qi, Z., Diao, X., Wang, Y., 2022. Genomic evidence for the recycling of complex organic carbon by novel thermoplasmatota clades in deep-sea sediments. *Msystems* 7 (3). https://doi.org/10.1002/bit.20347.

Zheng, Y., Feng, Z., Wang, P., Xu, S., Gao, X., Ren, L., Yang, T., Zhao, X., Wei, Y., Li, J., 2023. Suppressive performance of food waste composting with polylactic acid: Emphasis on microbial core metabolism pathways and mechanism. *Bioresour. Technol.* 384, 129339. https://doi.org/10.1016/J.BIORTECH.2023.129339.

Ziganshin, A.M., Ziganshina, E.E., Kleinsteuber, S., Nikolausz, M., 2016. Comparative analysis of methanogenic communities in different laboratory-scale anaerobic digesters. *Archaea* 2016. https://doi.org/10.1155/2016/3401272.